EFFECTS OF EARTHQUAKES
ON PARTIALLY-FILLED WATER TANKS

BY

Jun Koyama

Thesis submitted to the Faculty of the

Virginia Polytechnic Institute and State University

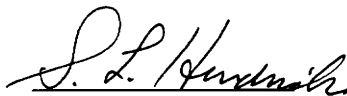in partial fulfilment of the requirements for the degree of
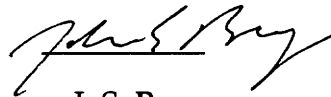
Master of Science

in

Engineering Mechanics

Approved:

L. Meirovitch

L. Meirovitch, Chairman

S. L. Hendricks

S. L. Hendricks

J. S. Bay

J. S. Bay

August 1994

Blacksburg, Virginia

ABSTRACT

This thesis is concerned with the effects of earthquakes on partially-filled water tanks. The analysis is applicable to rectangular water tanks, which have received little attention to date. The analysis is relatively involved and includes the derivation of the equations of motion for the vibration of the whole of tank by means of substructure synthesis, a stochastic analysis relating the random ground motion caused by earthquakes to the random vibration of the tank, a stochastic characterization of the fluid pressure and computation of the probability of failure of the tank.

ACKNOWLEDGMENTS

TABLE OF CONTENTS

LIST OF FIGURES

LIST OF TABLES

NOMENCLATURE

x, y, z	Cartesian coordinates for the tank
k_{ib}	Bending stiffness constants
k_{it}	Torsional stiffness constants
E	Young's modulus
v	Poisson's ratio
D	Plate flexural stiffness
T	Kinetic energy
m	Mass per unit area of plate
V	Potential energy
δW	Virtual work
$w(x,z,t)$	Plate displacement
$f(x,z,t)$	Nonconservative force density
$\phi_i(x,z)$	Admissible functions
$q_i(t)$	Generalized coordinates
ω_r	Natural frequencies
v_r	Eigenvectors
$\Phi(x,y,z,t)$	Velocity potential
c_p	Velocity of sound
ρ	Mass density of fluid
g	Gravitational constant
$\eta(x,z,t)$	Surface waveheight function
$p_o(x,z,t)$	Free surface pressure
l_n	Fluid velocity in the normal direction
a_i	Length of the tank in the horizontal direction
b	Height of the tank
Λ_n	Slosh frequencies

$x_i y_i z_i$	Local cartesian coordinates for the tank
I	Moment of inertia
R_c	Rigid-body displacement vector
x_c	Rigid-body displacement component along the x axis
y_c	Rigid-body displacement component along the y axis
R_i	Total displacement vector
R_{ci}	Radius vector from tank origin to the origin of the local axes
r_i	Radius vector from origin of the local axes to a typical point
s_i	Elastic displacement of a typical point
V_i	Total velocity of a point
V_{ci}	Rigid-body velocity
$\dot{s}_i$	Velocity of a typical point
$p_i(x_i, z_i, t)$	Distributed force
$\dot{S}$	Generalized force vector due to the rigid-body motion
P	Generalized force vector due to the fluid pressure
$E_{rib} I_{rib}$	Flexural rigidity of a rib
u_i	Modal vectors
$\eta_j(t)$	Modal coordinates
$F_j(t)$	Modal forces
$W_j(x, z)$	Eigenfunctions for the entire tank
$R_{F_j F_k}(\tau)$	Cross-correlation function between modal forces
$R_{f\hat{f}}(x, z, \hat{x}, \hat{z}, \tau)$	Distributed cross-correlation function between the distributed forces
$S_{F_j F_k}(\omega)$	Cross-spectral density function between modal forces
$S_{f\hat{f}}(x, z, \hat{x}, \hat{z}, \omega)$	Cross-spectral density function between the distributed foces
$R_{\sigma\hat{\sigma}}(x, z, \hat{x}, \hat{z}, \tau)$	Cross-correlation function between the principal stresses at x, y and $\hat{x}$, $\hat{y}$
$\sigma(x, z, t)$	Principal stress
$\Sigma_j(x, z)$	Spatial function of principal stress
$R_{\eta_j \eta_k}(\tau)$	Cross-correlation function between the modal coordinates

$g_j(t)$	Modal impulse response
$G_j(\omega)$	Modal frequency response
$S_{\eta_j \eta_k}(\omega)$	Cross-spectral density function between the modal coordinates
$\overline{G}_j(\omega)$	Complex conjugate of $G_j(\omega)$
$R_\sigma(x,z,\tau)$	Autocorrelation function of the principal stress
$p(\zeta,t)$	Fluid pressure distribution
$h(\zeta,t)$	Dynamic fluid pressure
ζ	Depth of the fluid measured from the surface
$R_{h\hat{h}}(\zeta,\hat{\zeta},\tau)$	Cross-correlation function between the dynamic fluid pressure at ζ and $\hat{\zeta}$
$S_{h\hat{h}}(\zeta,\hat{\zeta},\omega)$	Cross-spectral density function between the dynamic fluid pressure at ζ and $\hat{\zeta}$
$S_{h_x \hat{h}_x}(\zeta,\hat{\zeta},\omega)$	Cross-spectral density function between the dynamic fluid pressure action on panel A and C
$S_{h_y \hat{h}_y}(\zeta,\zeta,\omega)$	Cross-spectral density function between the dynamic fluid pressure action on panel B and D
$\Omega_n(\zeta)$	Shape of the fluid pressure
$H_n(\omega)$	Frequency response of the fluid pressure

1. INTRODUCTION

There have been many approaches to the analysis and design of fluid tanks, as described in Housner (ref. 1), Abramson (ref. 2), and Bauer et al (ref. 3). A great deal of research conducted in the last two decades on fluid/structure interaction for the purpose of developing new methods for analysis and design of flexible fluid tanks has been concerned mostly with cylindrical tanks.

In designing a water tank, the hydrodynamic loading is the most important factor. The hydrodynamic loading is strongly affected by the relation between the excitation frequencies and the natural frequencies of the structure. For most typical fluid tanks, fluid surface slosh occurs at frequencies that are much lower than those of the vibrating elastic tanks. As a result, for low excitation frequencies, such as in the case of seismic loading, the frequencies of the fluid slosh modes and the natural frequencies of the tank tend to be well separated. This suggests that the effects of fluid-structure interaction during vibration are minimal. Consequently, the fluid slosh forces exerted on the tank can be computed by regarding the tank walls as rigid.

To date, there seems to be no structural model for the full tank. The basic approach adopted here is a substructure synthesis (ref. 4), whereby a complex structure can be regarded as an assemblage of simpler substructures.

Many random phenomena exhibit statistical regularity. If the excitation exhibits statistical regularity, so does the response. In such cases it is more feasible to describe the excitation and response in terms of probability of occurrence rather than deterministically. We assume here that the random excitation is Gaussian, which permits us to use tools of random vibration to compute the probability of failure of the tank due to earthquake excitations.

This thesis covers the effect of earthquakes on partially filled rectangular water tanks. Modeling of the tank and of the fluid slosh is discussed in Chapter 2. Dynamics characteristics of the tank and fluid are derived in Chapter 3. Response of the tank to random excitation is discussed in Chapter 4. Numerical results are shown in Chapter 5. Chapter 6 contains conclusions and some suggestions for future work.

2. MODELING OF THE TANK AND OF THE FLUID SLOSH

2.1 Modeling Techniques

Perhaps the most widely used method for the analysis of complex structures is the finite element method. But, whereas the finite element method is very versatile in deriving algebraic eigenvalue problems for complex distributed-parameter structures, it has the major disadvantage that it often requires a very large number of degrees of freedom for accurate estimates of the lower natural frequencies and associated natural modes. In some cases, the required number of degrees of freedom is so large that other methods of analysis are recommended. This is often the case when the complex structure can be regarded as an assemblage of a small numbers of simple substructres. In this case, it is possible to construct a mathematical model with a substantially smaller number of degrees of freedom than the finite element method. One such method, developed by Hurty (ref. 5,6), has come to be known as component-mode synthesis. The question can be raised as to what constituted component-modes, but in general one can assume that they are generated by solving some form of substructure eigenvalue problem. In this regard, it should be noted that both the finite element method and the component-mode synthesis can be regarded as Rayleigh-Ritz methods. But, as pointed out by Meirovitch (ref. 7) and Meirovitch and Hale (ref. 8,9), in the spirit of Rayleigh-Ritz, one need use only admissible functions, as

long as the functions are from a complete set. Although substructure modes are certainly suitable admissible functions, they represent only a relatively small subset of the much broader set of admissible functions. To emphasize the mathematical requirement, and play down the physical implications of the term "component modes", we refer to the method whereby the structure is treated as an assemblage of substructures, each represented by a finite set of suitable admissible functions, as substructure synthesis.

2.2 Quasi-Comparison Functions

According to the Rayleigh-Ritz theory, in formulating the algebraic eigenvalue problem by rendering the quotient stationary, where the quotient is in terms of the energy inner product [W,W] instead of the inner product (W,$\mathcal{L}$W), the approximation can be constructed from the space of admissible fuctions rather than comparison functions (ref. 11). The main difference between admissible functions and comparison functions lies in the fact that admissible functions need satisfy only the geometric boundary conditions and the comparison functions must satisfy all the boundary conditions. Of course, there is also the question of differentiability, but in the classical Rayleigh-Ritz method this question seldom arises, as the functions used tend to have sufficient smoothness to ensure the existence of derivatives of high order.

In certain cases, by using admissible functions, the convergence is quite slow. On the other hand, the use of comparison functions yields relatively fast convergence. However, the fact that each of the comparison functions must satisfy all the boundary conditions can be quite a burden. To avoid these difficulties, a new class of admissible functions was introduced by Meirovitch

(ref. 10). This is the class of quasi-comparison functions defined as admissible functions of such a nature that finite linear combinations thereof are capable of satisfying the natural boundary conditions as accurately as desired. Hence, quasi-comparison functions are functions that individually act like admissible functions but in a finite group they behave more like comparison functions. In essence, quasi-comparison functions can be regarded as being complete in boundary conditions, in addition to being complete in energy.

2.3 Derivation of Quasi-Comparison Functions for the Tank
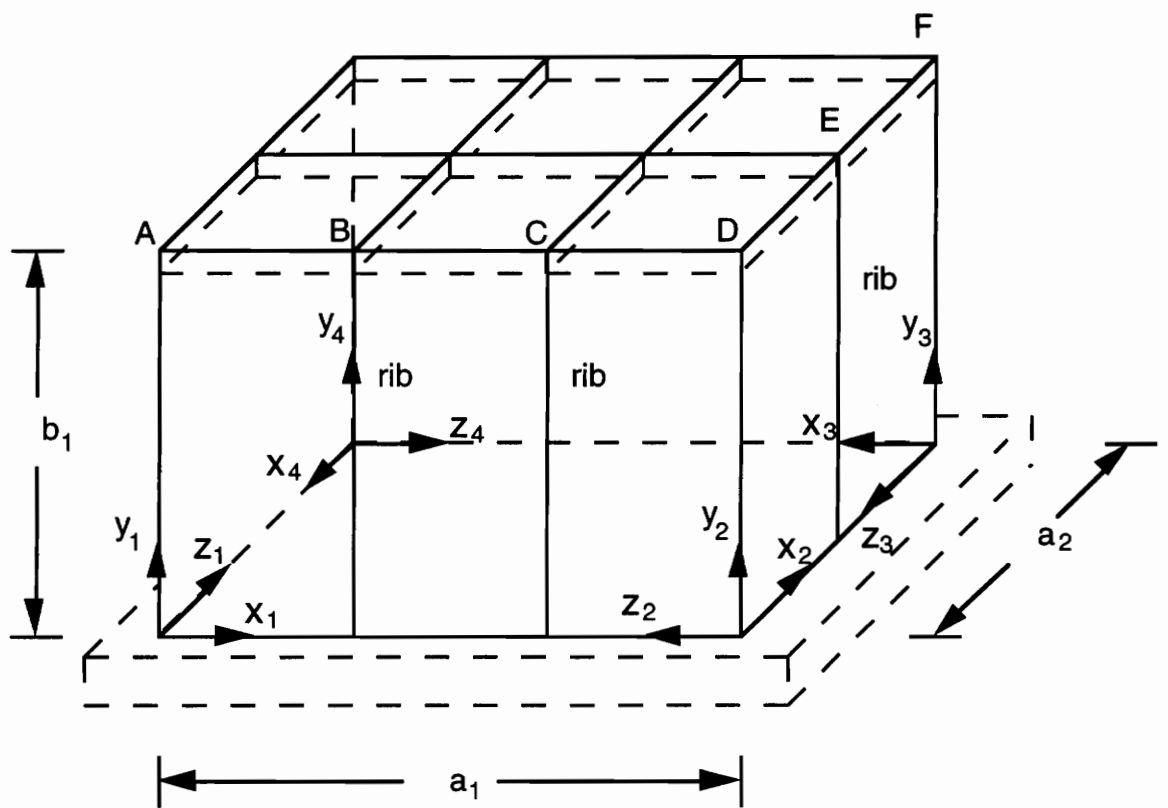
Figure 2.1 Configuration and coordinates of a water tank

The tank structure can be regarded as a box in the form of a parallelepiped

anchored to a foundation made of a concrete. Assuming that the foundation is rigid, the tank can be modeled as four vertical panels clamped at the bottom and with the sides connected to one another (Figure 2.1) so that the horizontal angle between any two adjacent panels remains 90 degree at all times. The top of the panel is reinforced by a bar, as shown in Figure 2.2. In addition, each of the panel
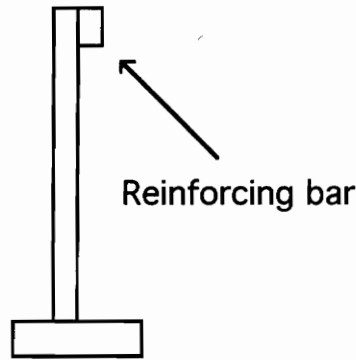
Figure 2.2 Bar at the top of the tank

is reinforced by one or two vertical ribs. It is assumed that the roof of the tank does not lend stiffness, so that it is not considered as a structural member. Hence, for the sake of this analysis, the box is regarded as open at the top. This is a conservative assumption, as a box clamped or simply-supported at the top is stiffer than an open one, albeit supported elastically by a bar.

We propose to model the tank structure by substructure synthesis (ref. 1). To this end, we use sets of local axes $x_i y_i z_i$ (i=1,2,3,4), as shown in Figure 2.1, where $y_1 = x_2$, $y_2 = x_3$, $y_3 = x_4$, $y_4 = x_1$, and $z_i = z$. We assume that the panels undergo bending deformations alone and that the displacement of a typical point on a panel can be expressed

$$w(x_i, z, t) = \sum_{r=1}^{n_r} \sum_{s=1}^{n_s} \phi_{rs}(x_i, z) q_{rs}(t), \quad i = 1,2,3,4 \tag{1}$$

where

$$\phi_{rs}(x_i, z) = \phi_r(x_i) \phi_s(z), \quad i = 1,2,3,4 \tag{2}$$

in which $\phi_r(x_i)$ and $\phi_s(z)$ are admissible functions (ref. 16), also known as shape functions. In particular, the admissible functions are chosen in the form of quasi-comparison functions, which are linear combinations of admissible functions capable of satisfying all the boundary conditions (ref. 11). As quasi-comparison functions in the y-direction, we choose a linear combination of clamped-clamped and clamped-free beam shape functions. The clamped-clamped shape functions have the expression

$$\phi_s(z) = \cos\beta_s z - \cosh\beta_s z - \frac{\sin\beta_s b - \sinh\beta_s b}{\cos\beta_s b - \cosh\beta_s b}(\sin\beta_s z - \sinh\beta_s z) \tag{3}$$

where $\beta_s b$ are roots of the characteristic equation

$$\cos\beta_s b \cosh\beta_s b = 1 \tag{4}$$

in which b is the height of the panel. Similarly, the clamped-free shape functions are given by

$$\phi_s(z) = \cos\beta_s z - \cosh\beta_s z + \frac{\sin\beta_s b - \sinh\beta_s b}{\cos\beta_s b + \cosh\beta_s b}(\sin\beta_s z - \sinh\beta_s z) \tag{5}$$

where $\beta_s b$ satisfy the characteristic equation

$$\cos\beta_s b \cosh\beta_s b = -1 \qquad\qquad (6)$$

The quasi-comparison functions $\phi_r(x_i)$ require a more elaborate discussion. To this end, we consider a rectangular frame in bending as shown in Figure 2.3, and propose to solve the eigenvalue problem for the frame. Then,
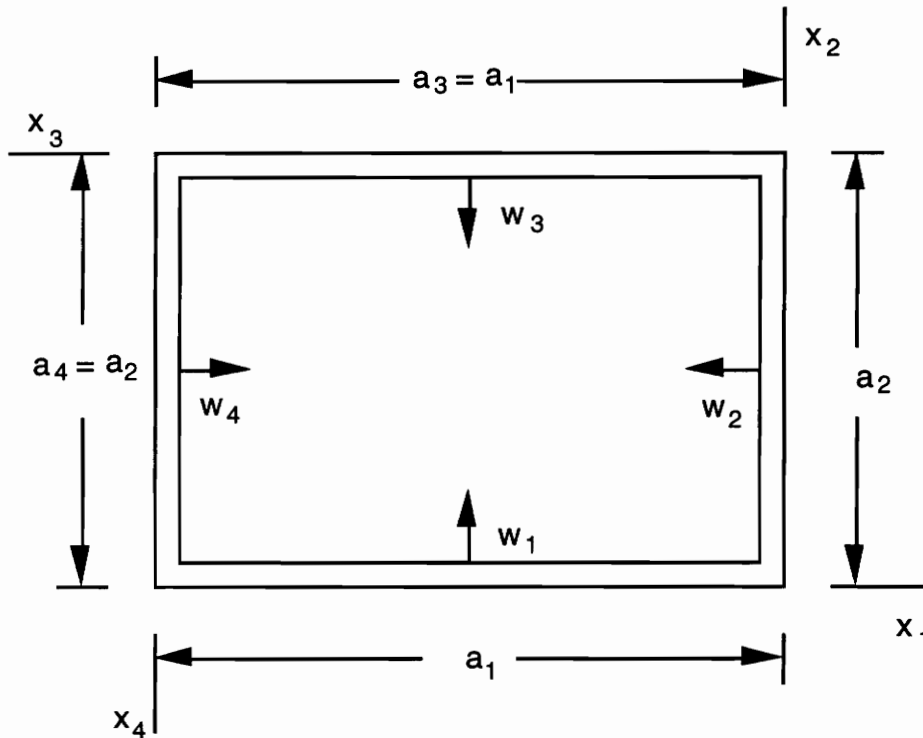

Figure 2.3 Rectangular frame in bending

the resulting eigenfunctions will be taken as quasi-comparison functions for the tank structure in the x-direction.

Assuming that the mass and stiffness distributions, m and EI, are the same for all sides, the eigenvalue problem can be defined as

$$\frac{d^4 w_i(x_i)}{dx_i^4} - \beta^4 w_i(x_i) = 0, \quad \beta^4 = \frac{m\omega^2}{EI}, \quad i = 1,2,3,4 \tag{7}$$

where w_i are subject to the boundary conditions

$$w_i(0) = w_i(a_i) = 0, \quad i = 1,2,3,4 \tag{8a}$$

$$\left.\frac{dw_4}{dx_4}\right|_{a_4} = \left.\frac{dw_1}{dx_1}\right|_0, \quad \left.\frac{dw_1}{dx_1}\right|_{a_1} = \left.\frac{dw_2}{dx_2}\right|_0, \quad \left.\frac{dw_2}{dx_2}\right|_{a_2} = \left.\frac{dw_3}{dx_3}\right|_0, \quad \left.\frac{dw_3}{dx_3}\right|_{a_3} = \left.\frac{dw_4}{dx_4}\right|_0 \tag{8b}$$

$$\left.\frac{d^2 w_4}{dx_4^2}\right|_{a_4} = \left.\frac{d^2 w_1}{dx_1^2}\right|_0, \quad \left.\frac{d^2 w_1}{dx_1^2}\right|_{a_1} = \left.\frac{d^2 w_2}{dx_2^2}\right|_0, \quad \left.\frac{d^2 w_2}{dx_2^2}\right|_{a_2} = \left.\frac{d^2 w_3}{dx_3^2}\right|_0, \quad \left.\frac{d^2 w_3}{dx_3^2}\right|_{a_3} = \left.\frac{d^2 w_4}{dx_4^2}\right|_0 \tag{8c}$$

The solution of Eqs. (7) can be written as

$$
\begin{aligned}
w_1(x_1) &= A_1 \sin\beta x_1 + A_2 \cos\beta x_1 + A_3 \sinh\beta x_1 + A_4 \cosh\beta x_1 \\
w_2(x_2) &= B_1 \sin\beta x_2 + B_2 \cos\beta x_2 + B_3 \sinh\beta x_2 + B_4 \cosh\beta x_2 \\
w_3(x_3) &= C_1 \sin\beta x_3 + C_2 \cos\beta x_3 + C_3 \sinh\beta x_3 + C_4 \cosh\beta x_3 \\
w_4(x_4) &= D_1 \sin\beta x_4 + D_2 \cos\beta x_4 + D_3 \sinh\beta x_4 + D_4 \cosh\beta x_4
\end{aligned} \tag{9}
$$

The problem can be simplified by observing that the structure is symmetric, so that the modes belong to two classes, symmetric and antisymmetric. In the case of symmetric modes, we have

$$w_3 = w_1, \quad w_4 = w_2 \tag{10}$$

resulting in

$$C_i = A_i, \quad D_i = B_i, \quad i = 1,2,3,4 \tag{11}$$

so that there are only eight unknown coefficients. Consistent with this, Eqs (8) reduce to

$$w_i(0) = w_i(a_i) = 0, \quad i = 1,2 \tag{12a}$$

$$\left.\frac{dw_2}{dx_2}\right|_{a_2} = \left.\frac{dw_1}{dx_1}\right|_0, \left.\frac{dw_1}{dx_1}\right|_{a_1} = \left.\frac{dw_2}{dx_2}\right|_0 \tag{12b}$$

$$\left.\frac{d^2w_2}{dx_2{}^2}\right|_{a_2} = \left.\frac{d^2w_1}{dx_1{}^2}\right|_0, \left.\frac{d^2w_1}{dx_1{}^2}\right|_{a_1} = \left.\frac{d^2w_2}{dx_2{}^2}\right|_0 \tag{12c}$$

Application of boundary conditions (12a) yields

$$w_1 = A_1(\sin\beta x_1 - \frac{\sin\beta a_1}{\sinh\beta a_1}\sinh\beta x_1)$$

$$+A_2(\cos\beta x_1 - \cosh\beta x_1 - \frac{\cos\beta a_1 - \cosh\beta a_1}{\sinh\beta a_1}\sinh\beta x_1)$$

$$w_2 = B_1(\sin\beta x_2 - \frac{\sin\beta a_2}{\sinh\beta a_2}\sinh\beta x_2) \tag{13}$$

$$+B_2(\cos\beta x_2 - \cosh\beta x_2 - \frac{\cos\beta a_2 - \cosh\beta a_2}{\sinh\beta a_2}\sinh\beta x_2)$$

Inserting Eqs. (13) into boundary conditions (12b) and (12c), we obtain

$$A_1(1 - \frac{\sin\beta a_1}{\sinh\beta a_1}) - A_2\frac{\cos\beta a_1 - \cosh\beta a_1}{\sinh\beta a_1} - B_1(\cos\beta a_2 - \frac{\sin\beta a_2}{\sinh\beta a_2}\cosh\beta a_2)$$

$$+B_2(\sin\beta a_2 + \sinh\beta a_2 + \frac{\cos\beta a_2 - \cosh\beta a_2}{\sinh\beta a_2}\cosh\beta a_2) = 0$$

$$A_1(\cos\beta a_1 - \frac{\sin\beta a_1}{\sinh\beta a_1}\cosh\beta a_1) - A_2(\sin\beta a_1 + \sinh\beta a_1 + \frac{\cos\beta a_1 - \cosh\beta a_1}{\sinh\beta a_1}\cosh\beta a_1)$$

$$\tag{14}$$

$$-B_1(1 - \frac{\sin\beta a_2}{\sinh\beta a_2}) + B_2 \frac{\cos\beta a_2 - \cosh\beta a_2}{\sinh\beta a_2} = 0$$

$$A_2 - B_1 \sin\beta a_2 - B_2 \cos\beta a_2 = 0$$

$$A_1 \sin\beta a_1 + A_2 \cos\beta a_1 - B_2 = 0$$

Equations (14) represent four homogeneous equations in the unknowns A_1, A_2, B_1, and B_2 and the parameter β. Equating the determinant of the coefficients to zero, we obtain a characteristic equation to be solved numerically for the eigenvalues $\beta_1, \beta_2, ...$ Then, inserting each of the eigenvalues into three of Eqs. (14) and letting one of the unknowns be equal to one, say $A_1 = 1$, it is possible to solve for the remaining three unknowns and the associated eigenvector. Upon inserting these values into Eqs. (10) and (13), we obtain the frame eigenfunctions.

In the case of antisymmetric modes, we have

$$w_3 = -w_1, w_4 = -w_2 \tag{15}$$

which implies that

$$C_i = -A_i, \quad D_i = -B_i, \quad i = 1,2,3,4 \tag{16}$$

Boundary conditions (12a) and Eqs. (13) retain their form. On the other hand, boundary conditions (12b) and (12c) are replaced by

$$-\frac{dw_2}{dx_2}\bigg|_{a_2} = \frac{dw_1}{dx_1}\bigg|_0, \frac{dw_1}{dx_1}\bigg|_{a_1} = \frac{dw_2}{dx_2}\bigg|_0 \tag{17a}$$

$$-\frac{d^2w_2}{dx_2{}^2}\bigg|_{a_2} = \frac{d^2w_1}{dx_1{}^2}\bigg|_0 , \frac{d^2w_1}{dx_1{}^2}\bigg|_{a_1} = \frac{d^2w_2}{dx_2{}^2}\bigg|_0 \qquad (17b)$$

Hence, inserting Eqs. (13) into Eqs. (17), we obtain

$$A_1(1-\frac{\sin\beta a_1}{\sinh\beta a_1}) - A_2\frac{\cos\beta a_1 - \cosh\beta a_1}{\sinh\beta a_1} + B_1(\cos\beta a_2 - \frac{\sin\beta a_2}{\sinh\beta a_2}\cosh\beta a_2)$$

$$-B_2(\sin\beta a_2 + \sinh\beta a_2 + \frac{\cos\beta a_2 - \cosh\beta a_2}{\sinh\beta a_2}\cosh\beta a_2) = 0$$

$$A_1(\cos\beta a_1 - \frac{\sin\beta a_1}{\sinh\beta a_1}\cosh\beta a_1) - A_2(\sin\beta a_1 + \sinh\beta a_1 + \frac{\cos\beta a_1 - \cosh\beta a_1}{\sinh\beta a_1}\cosh\beta a_1)$$

$$\qquad\qquad\qquad\qquad\qquad\qquad\qquad\qquad\qquad\qquad\qquad (18)$$

$$-B_1(1-\frac{\sin\beta a_2}{\sinh\beta a_2}) + B_2\frac{\cos\beta a_2 - \cosh\beta a_2}{\sinh\beta a_2} = 0$$

$$A_2 + B_1\sin\beta a_2 + B_2\cos\beta a_2 = 0$$

$$A_1\sin\beta a_1 + A_2\cos\beta a_1 - B_2 = 0$$

Of course, the procedure for evaluating A_1, A_2, B_1, B_2, and β remains the same.

Table 2.1 Eigenvalues of the rectangular frame

i	β_i	i	β_i
1	1.1982275	4	2.0545012
2	1.3698758	5	2.3130423
3	1.8078934	6	2.5334401

The symmetric and antisymmetric eigenfunctions of the rectangular frame will be used as the quasi-comparison functions $\phi_r(x_i)$ $(i=1,2,3,4; r=1,2,...,n_r)$ entering into Eq. (2). Equations (14) and (18) have been solved numerically and the six lowest eigenvalues and eigenfunctions are shown in Table 2.1 and Figures 2.4 and 2.5, respectively.
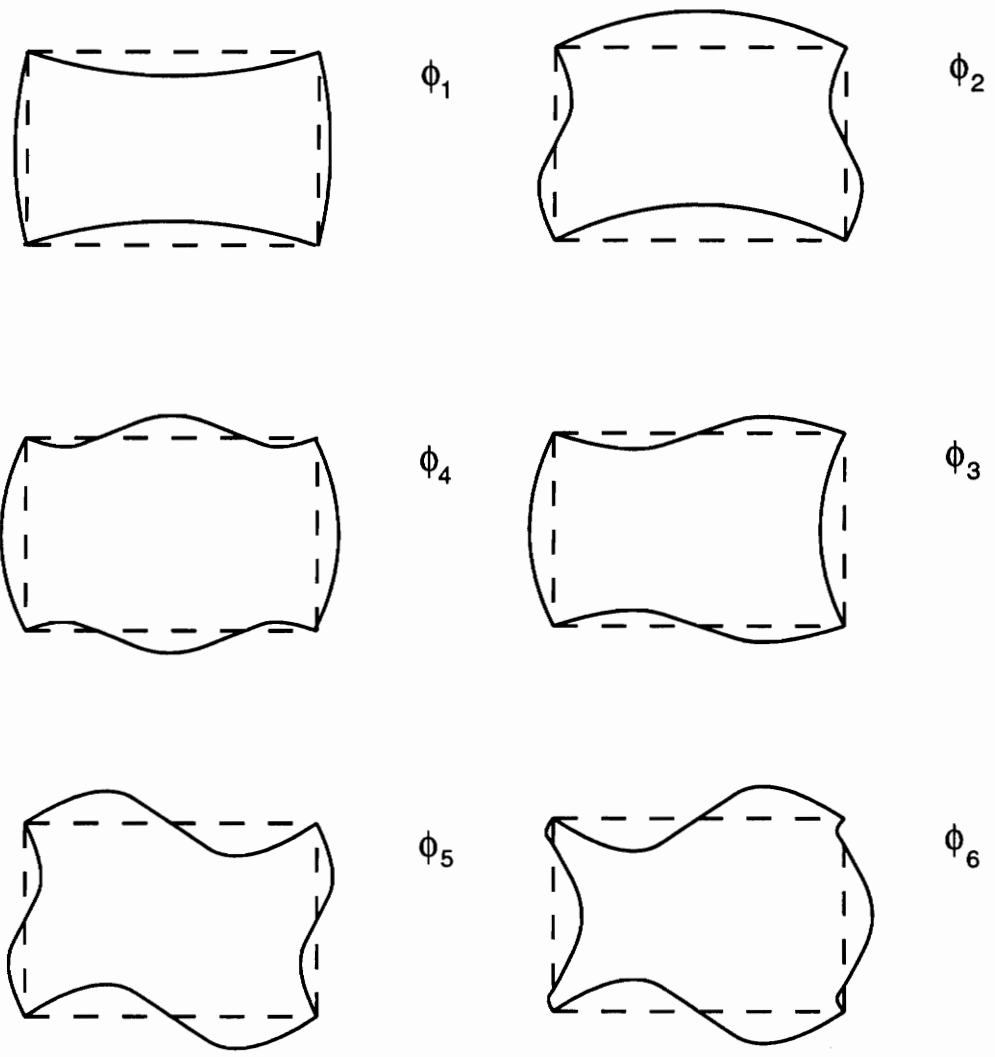
Figure 2.4 Symmetric frame modes   Figure 2.5 Antisymmetric frame modes

2.4 Distributed Spring Constants for the Reinforcing Bar at the Roof

We assume that the roof provides no structural support and that the upper edge of the walls is supported by a bar acting as a distributed spring both in bending and torsion (Figures 2.6 and 2.7).

The following expressions are used for the spring constant (ref. 17).

$$k_{1b1} = \frac{270 E I L^3}{x^2 (12x^4 - 114L^2x^2 + 180L^3x - 78L^4)} \tag{19a}$$

$$k_{1b2} = \frac{270 E I L^3}{x^2 (30x^4 - 90lx^3 + 48L^2x^2 + 54L^3x - 42L^4)} \tag{19b}$$

$$k_{2b} = \frac{24 E I L^3}{x^2 (x^4 - 10L^2x^2 + 16L^3x - 7L^4)} \tag{19c}$$

$$k_{1t} = k_{2t} = \frac{GL^3 \dfrac{ab^3}{3} \{1 - \dfrac{192}{\pi^5} \dfrac{b}{a} \tanh(\dfrac{\pi a}{2b})\}}{x(2L^2 + 3Lx - 6x^2)} \tag{19d}$$
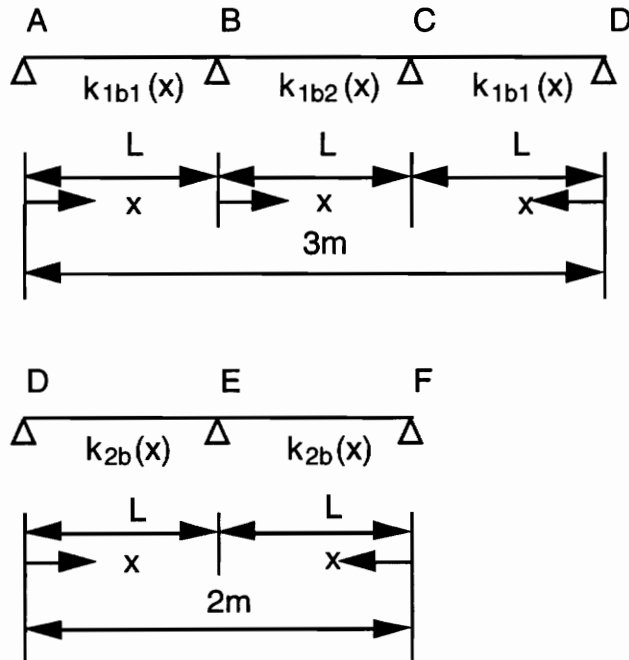
Figure 2.6 Boundary bending distributed spring
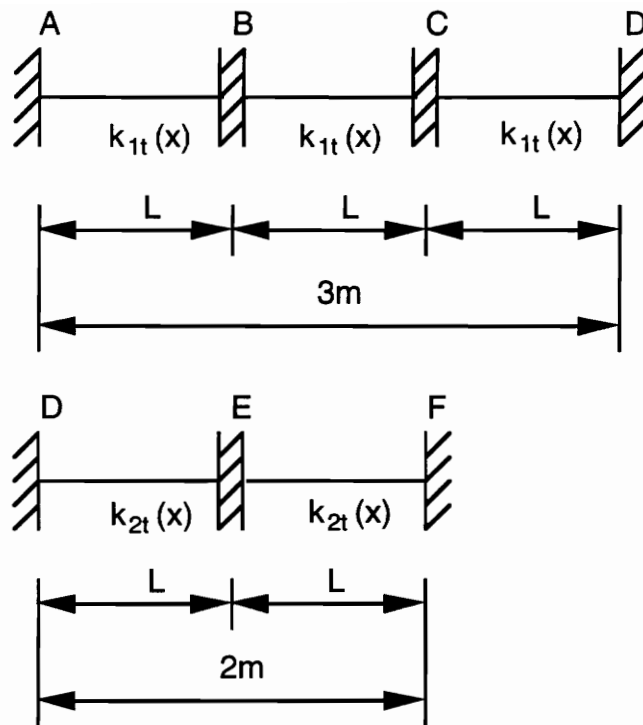
Figure 2.7 Boundary torsional distributed spring

where E, I, G, and L are Young's modulus, area moment of inertia, modulus of rigidity, and the length of the beam, respectivly.

3. DYNAMIC CHARACTERISTICS OF THE TANK AND FLUID

3.1 The Equations of Motion of the Tank

We assume that, due to ground motion, the tank experiences the rigid-body displacement

$$R_c = x_c i + y_c j \tag{20}$$

where x_c and y_c are assumed to be given. Hence, from Figure 3.1, we can write
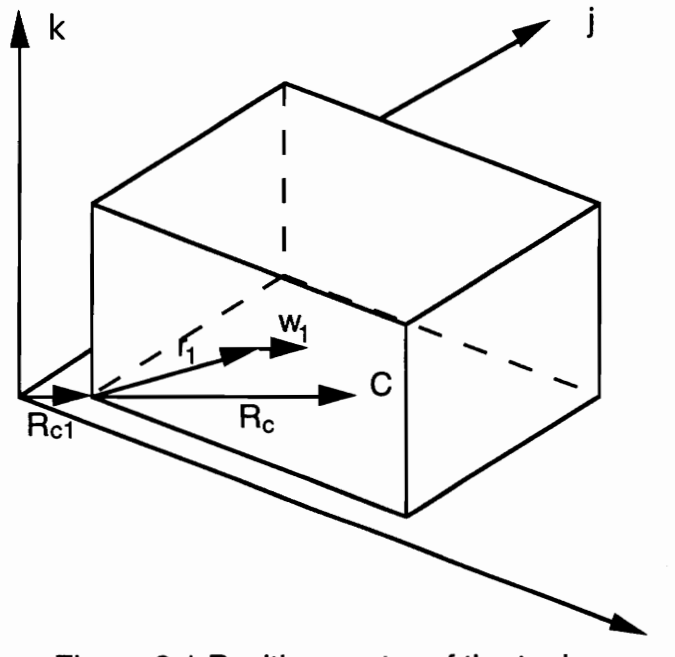
Figure 3.1 Position vector of the tank

the total position vector of a point on the tank in the form

$$R_i = R_{ci} + r_i + s_i \quad i = 1, 2, 3, 4 \tag{21}$$

in which

$$R_{c1} = R_c - \frac{a_1}{2}i - \frac{a_2}{2}j = (x_c - \frac{a_1}{2})i + (y_c - \frac{a_2}{2})j$$

$$R_{c2} = R_c + \frac{a_1}{2}i - \frac{a_2}{2}j = (x_c + \frac{a_1}{2})i + (y_c - \frac{a_2}{2})j$$

$$R_{c3} = R_c + \frac{a_1}{2}i + \frac{a_2}{2}j = (x_c + \frac{a_1}{2})i + (y_c + \frac{a_2}{2})j$$

$$\tag{22}$$

$$R_{c4} = R_c - \frac{a_1}{2}i + \frac{a_2}{2}j = (x_c - \frac{a_1}{2})i + (y_c + \frac{a_2}{2})j$$

$$r_1 = x_1 i + z_1 k, \ r_2 = x_2 j + z_2 k, \ r_3 = -x_3 i + z_3 k, \ r_4 = -x_4 j + z_4 k$$

$$s_1 = w_1 j, \ s_2 = -w_2 i, \ s_3 = -w_3 j, \ s_4 = w_4 i$$

The velocity vector of a point on the tank is

$$V_i = V_{ci} + \dot{s}_i, \quad i = 1, 2, 3, 4 \tag{23}$$

or more explicitly

$$V_1 = \dot{x}_c i + \dot{y}_c j + \dot{s}_1 j = \dot{x}_c i + (\dot{y}_c + \dot{s}_1)j$$

$$V_2 = \dot{x}_c i + \dot{y}_c j - \dot{s}_2 i = (\dot{x}_c - \dot{s}_2)i + \dot{y}_c j$$

$$V_3 = \dot{x}_c i + \dot{y}_c j - \dot{s}_3 j = \dot{x}_c i + (\dot{y}_c - \dot{s}_3)j \tag{24}$$

$$V_4 = \dot{x}_c i + \dot{y}_c j + \dot{s}_4 i = (\dot{x}_c + \dot{s}_4)i + \dot{y}_c j$$

The equation of motion can be obtained by means of the extended Hamilton's principle, or

$$\int_{t_1}^{t_2} (\delta T - \delta V + \delta W)dt = 0, \quad \delta w_i = 0, \quad i = 1,2,3,4, \quad t = t_1, t_2 \tag{25}$$

where T is the kinetic energy, V is the potential energy and δW is the virtual work. Using Eqs. (24), the kinetic energy can be written as

$$
\begin{aligned}
T &= \frac{1}{2}\sum_{i=1}^{4}\int_0^{a_i}\int_0^{b_i}\rho_i V_i V_i dx_i dz_i \\
&= \frac{1}{2}\int_0^{a_1}\int_0^{b}\rho[\dot{x}_c^2 + (\dot{y}_c + \dot{w}_1)^2]dx_1 dz_1 + \frac{1}{2}\int_0^{a_2}\int_0^{b}\rho[(\dot{x}_c - \dot{w}_2)^2 + \dot{y}_c^2]dx_2 dz_2 \\
&\quad + \frac{1}{2}\int_0^{a_3}\int_0^{b}\rho[\dot{x}_c^2 + (\dot{y}_c - \dot{w}_3)^2]dx_3 dz_3 + \frac{1}{2}\int_0^{a_4}\int_0^{b}\rho[(\dot{x}_c + \dot{w}_4)^2 + \dot{y}_c^2]dx_4 dz_4
\end{aligned}
\tag{26}
$$

The potential energy has the form

$$
\begin{aligned}
V &= \frac{1}{2}\sum_{i=1}^{4} D\int_0^{a_i}\int_0^{b_i}\{(\nabla^2 w_i)^2 + 2(1-\nu)[(\frac{\partial^2 w_i}{\partial x_i \partial z_i})^2 - \frac{\partial^2 w_i}{\partial x_i^2}\frac{\partial^2 w_i}{\partial z_i^2}]\}dx_i dz_i \\
&\quad + \frac{1}{2}\sum_{i=1}^{4}\int_0^{a_i}\{k_{ib}w_i^2(x_i,b_i,t) + k_{it}[\frac{\partial w_i(x_i,b_i,t)}{\partial x_i}]^2\}dx_i dz_i \\
&\quad + \frac{1}{2}\int_0^{b_1} E_{rib}I_{rib}(\frac{\partial^2 w_1}{\partial z_1^2})^2\Big|_{x=\frac{a_1}{3}} dz_1 + \frac{1}{2}\int_0^{b_1} E_{rib}I_{rib}(\frac{\partial^2 w_1}{\partial z_1^2})^2\Big|_{x=\frac{2a_1}{3}} dz_1 \\
&\quad + \frac{1}{2}\int_0^{b_2} E_{rib}I_{rib}(\frac{\partial^2 w_2}{\partial z_2^2})^2\Big|_{x=\frac{a_2}{2}} dz_2 + \frac{1}{2}\int_0^{b_3} E_{rib}I_{rib}(\frac{\partial^2 w_3}{\partial z_3^2})^2\Big|_{x=\frac{a_3}{3}} dz_3 \\
&\quad + \frac{1}{2}\int_0^{b_3} E_{rib}I_{rib}(\frac{\partial^2 w_3}{\partial z_3^2})^2\Big|_{x=\frac{2a_3}{3}} dz_3 + \frac{1}{2}\int_0^{b_4} E_{rib}I_{rib}(\frac{\partial^2 w_4}{\partial z_4^2})^2\Big|_{x=\frac{a_4}{2}} dz_4
\end{aligned}
\tag{27}
$$

where

$$D = \frac{Ed^3}{12(1-v^2)} \tag{28}$$

in which E is the modulus of elasticity, d is the wall thickness and v is the Poisson's ratio, ∇^2 is the Laplacian operator, k_{ib} are distributed spring constants in bending due to the reinforcing bar at the top of the wall, k_{it} are distributed torsional spring constraints of the same bar and E_{rib} I_{rib} are rib flexural rigidities. The virtual work is due to the distributed force $p_i(x_i, z_i, t)$ representing the fluid pressure in the tank and can be written as

$$\delta W = \sum_{i=1}^{4} \int_0^{a_i} \int_0^{b_i} p_i \delta w_i dx_i dz_i \tag{29}$$

Next, we assume that the elastic displacement can be expressed in the form

$$w(x, z, t) = \phi^T(x, z)q(t) \tag{30}$$

where $\phi(x,z)$ is a vector of quasi-comparison furctions and $q(t)$ is a vector of generalized coordinates. Implicit in Eq. (30) is the fact that the double subscript in Eq. (2) is replaced by a single subscript. Equation (30) is valid for all four panels, and in Eqs. (26), (27) and (29) we carried out integrations over the individual panels. In recognition of that, we express the displacements over each of the panels as follows:

$$w_i(x_i, z_i, t) = \phi^{(i)T}(x_i, z_i)q(t) \quad i = 1, 2, 3, 4 \tag{31}$$

where $\phi^{(i)}$ is the portion of ϕ that extends over panel i. Inserting Eqs. (31) into Eq. (26), we obtain the discretized kinetic energy

$$
\begin{aligned}
T = &\frac{1}{2}\int_0^{a_1}\int_0^b \rho(\dot{x}_c^2 + \dot{y}_c^2 + 2\dot{y}_c\phi^{(1)T}\dot{q} + \dot{q}^T\phi^{(1)}\phi^{(1)T}\dot{q})dx_1dz_1 \\
&+\frac{1}{2}\int_0^{a_2}\int_0^b \rho(\dot{x}_c^2 + \dot{y}_c^2 - 2\dot{x}_c\phi^{(2)T}\dot{q} + \dot{q}^T\phi^{(2)}\phi^{(2)T}\dot{q})dx_2dz_2 \\
&+\frac{1}{2}\int_0^{a_3}\int_0^b \rho(\dot{x}_c^2 + \dot{y}_c^2 - 2\dot{y}_c\phi^{(3)T}\dot{q} + \dot{q}^T\phi^{(3)}\phi^{(3)T}\dot{q})dx_3dz_3 \\
&+\frac{1}{2}\int_0^{a_4}\int_0^b \rho(\dot{x}_c^2 + \dot{y}_c^2 + 2\dot{x}_c\phi^{(4)T}\dot{q} + \dot{q}^T\phi^{(4)}\phi^{(4)T}\dot{q})dx_4dz_4 \\
= &\frac{1}{2}m(\dot{x}_c^2 + \dot{y}_c^2) + S^T\dot{q} + \frac{1}{2}\dot{q}^TM\dot{q}
\end{aligned}
\tag{32}
$$

where m is the total mass of the tank

$$
\begin{aligned}
S = &\dot{y}_c\left(\int_0^{a_1}\int_0^b \rho\phi^{(1)}dx_1dz_1 - \int_0^{a_3}\int_0^b \rho\phi^{(3)}dx_3dz_3\right) \\
&-\dot{x}_c\left(\int_0^{a_2}\int_0^b \rho\phi^{(2)}dx_2dz_2 - \int_0^{a_4}\int_0^b \rho\phi^{(4)}dx_4dz_4\right)
\end{aligned}
\tag{33}
$$

and

$$
M = \sum_{i=1}^{4}\int_0^{a_i}\int_0^{b_i} \rho\phi^{(i)}\phi^{(i)T}dx_idz_i
\tag{34}
$$

is a mass matrix. Introducing Eqs. (31) into Eq. (27), we obtain the discretized potential energy

$$
V = \frac{1}{2}q^TKq
\tag{35}
$$

where

$$
\begin{aligned}
K = \sum_{i=1}^{4} D \int_0^{a_i} \int_0^b & [\nabla^2 \phi^{(i)} \nabla^2 \phi^{(i)T} \\
& + (1-\nu)(2 \frac{\partial^2 \phi^{(i)}}{\partial x_i \partial z_i} \frac{\partial^2 \phi^{(i)T}}{\partial x_i \partial z_i} - \frac{\partial^2 \phi^{(i)}}{\partial x_i^2} \frac{\partial^2 \phi^{(i)T}}{\partial z_i^2} - \frac{\partial^2 \phi^{(i)}}{\partial z_i^2} \frac{\partial^2 \phi^{(i)T}}{\partial x_i^2})] dx_i dz_i \\
& + \int_0^{a_i} [k_{ib} \phi^{(i)}(x_i, b_i, t) \phi^{(i)T}(x_i, b_i, t) + k_{it} \frac{\partial \phi^{(i)}(x_i, b_i, t)}{\partial x_i} \frac{\partial \phi^{(i)T}(x_i, b_i, t)}{\partial x_i}] dx_i \\
& + E_{rib} I_{rib} \int_0^{b_1} \frac{\partial^2 \phi^{(1)}}{\partial z^2} \frac{\partial^2 \phi^{(1)T}}{\partial z^2} \bigg|_{x=\frac{a_1}{3}} + E_{rib} I_{rib} \int_0^{b_1} \frac{\partial^2 \phi^{(1)}}{\partial z^2} \frac{\partial^2 \phi^{(1)T}}{\partial z^2} \bigg|_{x=\frac{2a_1}{3}} \\
& + E_{rib} I_{rib} \int_0^{b_2} \frac{\partial^2 \phi^{(2)}}{\partial z^2} \frac{\partial^2 \phi^{(2)T}}{\partial z^2} \bigg|_{x=\frac{a_2}{2}} + E_{rib} I_{rib} \int_0^{b_3} \frac{\partial^2 \phi^{(3)}}{\partial z^2} \frac{\partial^2 \phi^{(3)T}}{\partial z^2} \bigg|_{x=\frac{a_3}{3}} \\
& + E_{rib} I_{rib} \int_0^{b_3} \frac{\partial^2 \phi^{(3)}}{\partial z^2} \frac{\partial^2 \phi^{(3)T}}{\partial z^2} \bigg|_{x=\frac{2a_3}{3}} + E_{rib} I_{rib} \int_0^{b_4} \frac{\partial^2 \phi^{(4)}}{\partial z^2} \frac{\partial^2 \phi^{(4)T}}{\partial z^2} \bigg|_{x=\frac{a_4}{2}}
\end{aligned}
\tag{36}
$$

Finally, insering Eqs. (31) into Eq. (29), we obtain the discretized virtual work

$$
\delta W = P^T \delta q
\tag{37}
$$

where

$$
P = -\sum_{i=1}^{4} \int_0^{a_i} \int_0^b p_i \phi^{(i)} dx_i dz_i
\tag{38}
$$

is the generalized force vector due to fluid pressure differential excluding static pressure. Introducing Eqs. (32), (35), and (37) into Eq. (25) and the following the usual steps, we obtain the equations of motion

$$M\ddot{q} + Kq = Q \tag{39}$$

where

$$Q = P - \dot{S} \tag{40}$$

is a generalized force vector due to the pressure differential in the tank and the rigid-body motion of the support.

3.2 The Tank Eigenvalue Problem

The equations of the motion for the tank are given by Eq. (39), with the force vector being given by Eq. (40), in which P is a force vector due to the fluid pressure differential in the tank and $-\dot{S}$ is an inertial force vector due to the ground motion, both forces assumed to represent random processes. To obtain the solution of Eq. (39), we first solve the eigenvalue problem

$$Ku = \omega^2 Mu \tag{41}$$

where K and M are real symmetric matrices. The solution consists of the eigenvalues ω_j^2 and eigenvectors u_j (j=1,2,...,n), where ω_j are recognized as the natural frequencies of the tank and u_j are the associated modal vectors; n is the number of degrees of freedom of the discretized tank. The modal vectors are orthogonal and are normalized so as to satisfy

$$u_k{}^T Mu_j = \delta_{jk}, \quad u_k{}^T Ku_j = \omega_j^2 \delta_{jk} \quad j,k = 1,2,...,n \tag{42}$$

where δ_{jk} is the Kronecker delta. Then, the solution of Eq. (39) can be expressed in the form of the linear combination

$$q(t) = \sum_{j=1}^{n} \eta_j(t)u_j \tag{43}$$

where $\eta_j(t)$ are modal coordinates. Introducing Eq. (43) into Eq. (39), premultiplying both sides of the resulting equation by u_k^T and using Eq. (42), we obtain the set of independent modal equations

$$\ddot{\eta}_j(t) + \omega_j^2 \eta(t) = F_j(t), \quad j = 1, 2, \ldots, n \tag{44}$$

where $F_j(t)$ are modal forces. Before discussing the modal forces, we wish to establish the relation between the actual displacements and the modal displacements. The actual displacement is

$$w(x, z, t) = \phi^T(x, z)q(t) \tag{45}$$

where $\phi(x, z)$ is a vector of quasicomparison functions and $q(t)$ is a vector of generalized coordinates. Now, we insert Eq. (43) into Eq. (45) and write

$$w(x, z, t) = \phi^T(x, z)q(t) = \phi^T(x, z)\sum_{j=1}^{n} \eta_j(t)u_j = \sum_{j=1}^{n} W_j(x, z)\eta_j(t) \tag{46}$$

in which

$$W_j(x,z) = \phi^T(x,z)u_j, \quad j = 1,2,\ldots,n \tag{47}$$

are recognized as the eigenfunctions for the full tank structure.

To determine the modal forces, we denote by f(x,z,t) the force density at any point on the tank, and we observe that f contains contributions from the fluid pressure differential and the ground motion. Then, using Eq. (43) and Eq. (46), we can write the virtual work as

$$\begin{aligned}
\delta W &= \int_0^a\int_0^b f(x,z,t)\delta w(x,z,t)dxdz \\
&= \int_0^a\int_0^b f(x,z,t)\sum_{j=1}^n W_j(x,z)\delta\eta_j(t)dxdz = \\
&= \sum_{j=1}^n F_j(t)\delta\eta_j(t)
\end{aligned} \tag{48}$$

where

$$F_j(t) = \int_0^a\int_0^b f(x,z,t)W_j(x,z)dxdz \tag{49}$$

are the modal forces. As a matter of interest, we wish to relate f(x,z,t) to the generalized force vector Q, Eq. (40). To this end, we use Eq. (43) and write the virtual work in the form

$$\delta W = Q^T\delta q = Q^T\sum_{j=1}^n \delta\eta_j(t)u_j = \sum_{j=1}^n Q^Tu_j\delta\eta_j \tag{50}$$

so that the desired relation is

$$F_j(t) = Q^T u_j = \int_0^a \int_0^b f(x,z,t) W_j(x,z) dx dz \tag{51}$$

3.3 Fluid Slosh Frequencies and Relation to Tank Frequencies

Under the assumption of small displacements, the velocity potential $\Phi(x,y,z,t)$ for the motion of a inviscid fluid satisfies the wave equation (ref.13)

$$\nabla^2 \Phi = \frac{1}{c_p^2} \frac{\partial^2 \Phi}{\partial t^2} \tag{52}$$

where c_p is the sound velocity and ∇^2 is the three-dimensional Laplacian operator defined as

$$\nabla^2 = \frac{\partial^2}{\partial x^2} + \frac{\partial^2}{\partial y^2} + \frac{\partial^2}{\partial z^2} \tag{53}$$

For low frequencies, the fluid can be assumed to be incompressible. As a result, the governing equation for the velocity potential, Eq. (52) simplifies to the Laplace equation

$$\nabla^2 \Phi = 0 \tag{54}$$

Moreover, the pressure $p(x,y,z,t)$ is governed by the linearized Bernoulli equation

$$\frac{\partial \Phi}{\partial t} + \frac{1}{\rho} p + gz = 0 \tag{55}$$

where ρ is the mass density of the fluid and g is the gravitational constant. The velocity potential representing a solution of Eq. (55) must satisfy given boundary conditions. The free surface condition requires that no fluid particle leave the surface. In terms of the waveheight function $\eta(x,y,t)$ of the surface, the following boundary conditions apply

$$\frac{\partial \eta}{\partial t} - \frac{\partial \Phi}{\partial z} = 0 \tag{56}$$

$$\frac{\partial \Phi}{\partial t} + \frac{1}{\rho} p_0 + g\eta = 0 \tag{57}$$

where $p_0(x,y,t)$ is the free surface pressure. At any point of contact between the fluid and structure, the normal component of the fluid velocity must be equal to the structure velocity, or

$$\frac{\partial \Phi}{\partial n} = l_n \tag{58}$$

where n is the normal direction. For a rigid rectangular tank of dimensions a_1, a_2, and b, the mode shapes η_{mn} and natural frequencies Λ_{mn} of the free surface waveheight η are given by (ref. 13)

$$\eta_{mn} = \sum_{m=0}^{\infty} \sum_{n=0}^{\infty} A_{mn} \cos\frac{m\pi}{2a_1}(2x + a_1) \cos\frac{n\pi}{2a_2}(2y + a_2) \tag{59}$$

$$\Lambda_{mn}^2 = gk_{mn} \tanh(k_{mn}h) \tag{60}$$

where the constant k_{mn} is defined by

$$k_{mn}^2 = (\frac{m^2}{a_1{}^2} + \frac{n^2}{a_2{}^2})\pi^2 \tag{61}$$

and h is the height of the fluid. When the excitation is parallel to the x-axis, the natural frequency Λ_n of the nth mode of the free surface waveheight can be obtained from

$$\Lambda_n^2 = \frac{(2n+1)\pi}{a_1} g \tanh \frac{(2n+1)\pi}{a_1} h \tag{62}$$

4. RESPONSE OF THE TANK TO RANDOM EXCITATION

4.1 The Principal Stresses Probability Density Function

We define the cross-correlation function between modal forces (ref. 12) as follows:

$$
\begin{aligned}
R_{F_j F_k}(\tau) &= \lim_{T \to \infty} \frac{1}{T} \int_{-\frac{T}{2}}^{\frac{T}{2}} F_j(t) F_k(t+\tau) dt \\
&= \lim_{T \to \infty} \frac{1}{T} \int_{-\frac{T}{2}}^{\frac{T}{2}} [\int_0^a \int_0^b f(x,z,t) W_j(x,z) dx dz][\int_0^a \int_0^b f(\hat{x},\hat{z},t) W_k(\hat{x},\hat{z}) d\hat{x} d\hat{z}] dt \\
&= \int_0^a \int_0^b W_j(x,z) \{ \int_0^a \int_0^b W_k(\hat{x},\hat{z})[\lim_{T \to \infty} \frac{1}{T} \int_{-\frac{T}{2}}^{\frac{T}{2}} f(x,z,t) f(\hat{x},\hat{z},t) dt] d\hat{x} d\hat{z} \} dx dz \\
&= \int_0^a \int_0^b \int_0^a \int_0^b W_j(x,z) W_k(\hat{x},\hat{z}) R_{f\hat{f}}(x,z,\hat{x},\hat{z},\tau) d\hat{x} d\hat{z} dx dz \qquad (63)
\end{aligned}
$$

where

$$
R_{f\hat{f}}(x,z,\hat{x},\hat{z},\tau) = \lim_{T \to \infty} \frac{1}{T} \int_{-\frac{T}{2}}^{\frac{T}{2}} f(x,z,t) f(\hat{x},\hat{z},t) dt \qquad (64)
$$

is the distributed cross-correlation function between the distributed forces $f(x,z,t)$ and $f(\hat{x},\hat{z},t)$. The cross-spectral density function is defined as the Fourier transform of $R_{f\hat{f}}$, or

$$S_{F_jF_k}(\omega) = \int_{-\infty}^{\infty} R_{F_jF_k} e^{-i\omega\tau} d\tau$$

$$= \int_{-\infty}^{\infty} [\int_0^a \int_0^b \int_0^a \int_0^b W_j(x,z)W_k(\hat{x},\hat{z}) R_{f\hat{f}}(x,z,\hat{x},\hat{z},\tau) d\hat{x}d\hat{z}dxdz] e^{-i\omega\tau} d\tau$$

$$= \int_0^a \int_0^b \int_0^a \int_0^b W_j(x,z)W_k(\hat{x},\hat{z}) [\int_{-\infty}^{\infty} R_{f\hat{f}}(x,z,\hat{x},\hat{z},\tau) e^{-i\omega\tau} d\tau] d\hat{x}d\hat{z}dxdz$$

$$= \int_0^a \int_0^b \int_0^a \int_0^b W_j(x,z)W_k(\hat{x},\hat{z}) S_{f\hat{f}}(x,z,\hat{x},\hat{z},\omega) d\hat{x}d\hat{z}dxdz \tag{65}$$

where

$$S_{f\hat{f}}(x,z,\hat{x},\hat{z},\omega) = \int_{-\infty}^{\infty} R_{f\hat{f}}(x,z,\hat{x},\hat{z},\tau) e^{-i\omega\tau} d\tau \tag{66}$$

is the distributed cross-spectral density function between the excitation process $f(x,z,t)$ and $f(\hat{x},\hat{z},t)$.

The cross-correlation function between the principal stress at x, z and $\hat{x}$, $\hat{z}$ has the form

$$R_{\sigma\hat{\sigma}}(x,z,\hat{x},\hat{z},\tau) = \lim_{T\to\infty} \frac{1}{T} \int_{-\frac{T}{2}}^{\frac{T}{2}} \sigma(x,z,t)\sigma(\hat{x},\hat{z},t+\tau)dt$$

$$= \lim_{T\to\infty} \frac{1}{T} \int_{-\frac{T}{2}}^{\frac{T}{2}} [\sum_{j=1}^n \Sigma_j(x,z)\eta_j(t)][\sum_{k=1}^n \Sigma_k(\hat{x},\hat{z})\eta_k(t+\tau)]dt$$

$$= \sum_{j=1}^n \sum_{k=1}^n \Sigma_j(x,z)\Sigma_k(\hat{x},\hat{z})R_{\eta_j\eta_k}(\tau) \tag{67}$$

in which

$$\sigma(x,z,t) = \frac{3D}{d^2}[(1+v)(\frac{\partial^2 w(x,z,t)}{\partial x^2} + \frac{\partial^2 w(x,z,t)}{\partial z^2})$$

$$+(1-v)\sqrt{(\frac{\partial^2 w(x,z,t)}{\partial x^2}-\frac{\partial^2 w(x,z,t)}{\partial z^2})^2+4(\frac{\partial^2 w(x,z,t)}{\partial x \partial z})^2}] \tag{68a}$$

$$\Sigma_j(x,z)=\frac{3D}{d^2}[(1+v)(\frac{\partial^2 W_j(x,z)}{\partial x^2}+\frac{\partial^2 W_j(x,z)}{\partial z^2})$$

$$+(1-v)\sqrt{(\frac{\partial^2 W_j(x,z)}{\partial x^2}-\frac{\partial^2 W_j(x,z)}{\partial z^2})^2+4(\frac{\partial^2 W_j(x,z)}{\partial x \partial z})^2}] \tag{68b}$$

$$R_{\eta_j \eta_k}=\lim_{T\to\infty}\frac{1}{T}\int_{-\frac{T}{2}}^{\frac{T}{2}}\eta_j(t)\eta_k(t+\tau)dt \tag{68c}$$

where D is the flexural rigidity of the plate, and d is the thickness of the plate.

At this point, we wish to relate the principal stresses cross-correlation function with the excitation cross-spectral density function. To this end, we denote the modal impulse response by $g_j(t)$ and the modal frequency response by $G_j(\omega)$, where from Eq. (44)

$$G_j(\omega)=\frac{1}{\omega_j^2-\omega^2}, \quad j=1,2,...,n \tag{69}$$

The frequency response is related to the impulse response by the convolution integral

$$\eta_j(t)=\int_{-\infty}^{\infty}g_j(\mu_j)F_j(t-\mu_j)d\mu_j, \quad j=1,2,...,n \tag{70}$$

where μ_j is a dummy variable. Inserting Eq. (70) into Eq. (68), we obtain

$$R_{\eta_j \eta_k}(\tau)=\lim_{T\to\infty}\frac{1}{T}\int_{-\frac{T}{2}}^{\frac{T}{2}}[\int_{-\infty}^{\infty}g_j(\mu_j)F_j(t-\mu_j)d\mu_j][\int_{-\infty}^{\infty}g_k(\mu_k)F_k(t+\tau-\mu_k)d\mu_k]dt$$

$$= \int_{-\infty}^{\infty} \int_{-\infty}^{\infty} g_j(\mu_j) g_k(\mu_k) [\lim_{T\to\infty} \frac{1}{T} F_j(t-\mu_j) F_k(t+\tau-\mu_k) dt] d\mu_j d\mu_k \quad (71)$$

Assuming that the excitation is ergodic, and hence stationary, and using Eq. (63), we can write

$$\lim_{T\to\infty} \frac{1}{T} \int_{-\frac{T}{2}}^{\frac{T}{2}} F_j(t-\mu_j) F_k(t+\tau-\mu_k) dt = \lim_{T\to\infty} \frac{1}{T} \int_{-\frac{T}{2}}^{\frac{T}{2}} F_j(t) F_k(t+\tau+\mu_j-\mu_k) dt$$

$$= R_{F_j F_k}(t+\mu_j-\mu_k) \quad (72)$$

so that Eq. (71) becomes

$$R_{\eta_j \eta_k}(\tau) = \int_{-\infty}^{\infty} \int_{-\infty}^{\infty} g_j(\mu_j) g_k(\mu_k) R_{F_j F_k}(\tau+\mu_j-\mu_k) d\mu_j d\mu_k \quad (73)$$

which relates the cross-correlation functions of the principal stress to the cross-correlation functions of the modal excitations.

Next, we write the cross-spectral density function associated with the modal response of the Fourier transform

$$S_{\eta_j \eta_k}(\omega) = \int_{-\infty}^{\infty} R_{\eta_j \eta_k}(\tau) e^{-i\omega\tau} d\tau$$

$$= \int_{-\infty}^{\infty} e^{-i\omega\tau} [\int_{-\infty}^{\infty} \int_{-\infty}^{\infty} g_j(\mu_j) g_k(\mu_k) R_{F_j F_k}(\tau+\mu_j-\mu_k) d\mu_j d\mu_k] d\tau \quad (74)$$

Moreover, $R_{F_j F_k}$ be expressed as the inverse Fourier transform

$$R_{F_j F_k}(\tau+\mu_j-\mu_k) = \frac{1}{2\pi} \int_{-\infty}^{\infty} S_{F_j F_k}(\omega) e^{i\omega(\tau+\mu_j-\mu_k)} d\omega \quad (75)$$

where $S_{F_j F_k}$ is the cross-spectral density function associated with the modal excitation process $F_j(t)$ and $F_k(t)$. Inserting Eq. (75) into Eq. (74) and considering Eq. (69), we can write

$$
\begin{aligned}
S_{\eta_j \eta_k}(\omega) &= \int_{-\infty}^{\infty} e^{-i\omega\tau} \{ \int_{-\infty}^{\infty} \int_{-\infty}^{\infty} g_j(\mu_j) g_k(\mu_k) [\frac{1}{2\omega} \int_{-\infty}^{\infty} S_{F_j F_k}(\omega) e^{i\omega(\tau+\mu_j-\mu_k)} d\omega] d\mu_j d\mu_k \} d\tau \\
&= \int_{-\infty}^{\infty} e^{-i\omega\tau} \{ \frac{1}{2\omega} \int_{-\infty}^{\infty} S_{F_j F_k}(\omega) [\int_{-\infty}^{\infty} g_j(\mu_j) e^{i\omega\mu_j} d\mu_j \int_{-\infty}^{\infty} g_k(\mu_k) e^{-i\omega\mu_k} d\mu_k] e^{i\omega\tau} d\omega \} d\tau \\
&= \int_{-\infty}^{\infty} e^{-i\omega\tau} [\frac{1}{2\omega} \int_{-\infty}^{\infty} \overline{G}_j(\omega) G_k(\omega) S_{F_j F_k}(\omega) e^{i\omega\tau} d\omega] d\tau
\end{aligned}
\tag{76}
$$

where $\overline{G}_j(\omega) = G_j(-\omega)$ is the complex conjugate of $G_j(\omega)$. Comparing Eq. (74) and Eq. (76) and recognizing that the modal response cross-correlation function $R_{\eta_j \eta_k}(\tau)$ must be equal to the inverse Fourier transform of the modal response cross-spectral density function $S_{\eta_j \eta_k}(\omega)$, we conclude that

$$
S_{\eta_j \eta_k}(\omega) = \overline{G}_j(\omega) G_k(\omega) S_{F_j F_k}(\omega)
\tag{77}
$$

and

$$
\begin{aligned}
R_{\eta_j \eta_k}(\tau) &= \frac{1}{2\pi} \int_{-\infty}^{\infty} S_{\eta_j \eta_k}(\omega) e^{i\omega\tau} d\omega \\
&= \frac{1}{2\pi} \int_{-\infty}^{\infty} \overline{G}_j(\omega) G_k(\omega) S_{F_j F_k}(\omega) e^{i\omega\tau} d\omega
\end{aligned}
\tag{78}
$$

represent a Fourier transform pair. Inserting Eq. (78) into Eq. (67), we obtain the cross-correlation function between the principal stress at x, z and $\hat{x}$, $\hat{z}$ in the form

$$R_{\sigma\hat{\sigma}}(x,z,\hat{x},\hat{z},\tau) = \frac{1}{2\pi}\sum_{j=1}^{n}\sum_{k=1}^{n}\Sigma_{j}(x,z)\Sigma_{k}(\hat{x},\hat{z})\int_{-\infty}^{\infty}\overline{G}_{j}(\omega)G_{k}(\omega)S_{F_{j}F_{k}}e^{i\omega\tau}d\omega \qquad (79)$$

where the modal excitation cross-spectral density function $S_{F_{j}F_{k}}(\omega)$ is related to the actual excitation cross-spectral density function $S_{\hat{f}\hat{f}}(x,z,\hat{x},\hat{z},\omega)$ by Eq. (65).

For $\hat{x}=x$, $\hat{z}=z$, the principal stresses cross-correlation function, Eq. (79) reduces to the principal stresses autocorrelation function

$$R_{\sigma}(x,z,\tau) = \frac{1}{2\pi}\sum_{j=1}^{n}\sum_{k=1}^{n}\Sigma_{j}(x,z)\Sigma_{k}(x,z)\int_{-\infty}^{\infty}\overline{G}_{j}(\omega)G_{k}(\omega)S_{F_{j}F_{k}}e^{i\omega\tau}d\omega \qquad (80)$$

Finally, letting t=0 in Eq. (80), we obtain the principal stresses mean square value

$$R_{\sigma}(x,z,0) = \frac{1}{2\pi}\sum_{j=1}^{n}\sum_{k=1}^{n}\Sigma_{j}(x,z)\Sigma_{k}(x,z)\int_{-\infty}^{\infty}\overline{G}_{j}(\omega)G_{k}(\omega)S_{F_{j}F_{k}}d\omega \qquad (81)$$

The square root of $\sigma(x,z,0)$ is the standard deviation associated with the probability density function of $\sigma(x,z,t)$. Hence, for a given actual excitation cross-spectral density function $S_{\hat{f}\hat{f}}(x,z,\hat{x},\hat{z},\omega)$, Eq. (65) yields the modal excitation cross-spectral function $S_{F_{j}F_{k}}(\omega)$, which can be used in conjunction with Eq. (81) to compute the principal stresses mean square value, thus defining the principal stresses probability density function. That permits us to predict the probability of failure of the tank by using maximum principal stress theory (ref. 14).

4.2 Spectral Densities for the Fluid Pressure

The velocity potential $\Phi(x,y,z,t)$ and fluid pressure $p(x,y,z,t)$ can be obtained from Eq. (56) - (58). The fluid pressure distribution $p(\zeta,t)$ on a given wall can be expressed as

$$p(\zeta,t) = -\rho g\zeta + h(\zeta,t) \tag{82}$$

where ρg is the weight density of the fluid, $h(\zeta,t)$ is the dynamic fluid pressure and ζ is the depth of the fluid measured from the free surface.

For a stationary random process, the cross-correlation function $R_{h\hat{h}}(\zeta,\hat{\zeta},\tau)$ is given by

$$R_{h\hat{h}}(\zeta,\hat{\zeta},\tau) = \lim_{T\to\infty} \frac{1}{T} \int_{-\frac{T}{2}}^{\frac{T}{2}} h(\zeta,t)h(\hat{\zeta},t+\tau)dt \tag{83}$$

and the cross-spectral density $S_{h\hat{h}}(\zeta,\hat{\zeta},\omega)$ is

$$S_{h\hat{h}}(\zeta,\hat{\zeta},\omega) = \int_{-\infty}^{\infty} R_{h\hat{h}}(\zeta,\hat{\zeta},\tau)e^{-i\omega\tau}d\tau \tag{84}$$

Consequently, the cross-correlation function $R_{h\hat{h}}(\zeta,\hat{\zeta},\tau)$ can also be obtained by taking the inverse Fourier transform of the cross-spectral density $S_{h\hat{h}}(\zeta,\hat{\zeta},\omega)$ as follows

$$R_{h\hat{h}}(\zeta,\hat{\zeta},\tau) = \frac{1}{2\pi} \int_{-\infty}^{\infty} S_{h\hat{h}}(\zeta,\hat{\zeta},\omega)e^{i\omega\tau}d\tau \tag{85}$$

When the tank is subjected to stationary random excitations in the directions parallel to the x-axis and the y-axis, the power spectral densities of the dynamic fluid pressure $S_{h_x \hat{h}_x}(\zeta, \hat{\zeta}, \omega)$ acting on walls A and C (normal to the x-axis) and $S_{h_y \hat{h}_y}(\zeta, \hat{\zeta}, \omega)$ acting on walls B and D (normal to the y-axis) are given by

$$S_{h_x \hat{h}_x}(\zeta, \hat{\zeta}, \omega) = [\sum_{n=0}^{\infty} \sum_{m=0}^{\infty} \Omega_{xn}(\zeta) \Omega_{xm}(\hat{\zeta}) H_{xn}(\omega) H_{xm}(\omega)] S_{\ddot{x}_c}(\omega) \qquad (86a)$$

$$S_{h_y \hat{h}_y}(\zeta, \hat{\zeta}, \omega) = [\sum_{n=0}^{\infty} \sum_{m=0}^{\infty} \Omega_{yn}(\zeta) \Omega_{ym}(\hat{\zeta}) H_{yn}(\omega) H_{ym}(\omega)] S_{\ddot{y}_c}(\omega) \qquad (86b)$$

where $\Omega_n(\zeta)$ and $H_n(\omega)$ are the shape and frequency response of the nth normal mode of the fluid pressure, respectively, and $S_{\ddot{x}_c}(\omega)$ and $S_{\ddot{y}_c}(\omega)$ are the power spectral densities for the base accelerations $\ddot{x}_c$ and $\ddot{y}_c$ in the x- and y-directions, respectively. The functions $\Omega_n(\zeta)$ and $H_n(\omega)$ are defined as

$$\Omega_{xn}(\zeta) = \frac{4a_1}{\pi^2(2n+1)^2} \frac{\cosh \frac{(2n+1)\pi}{a_1}(\zeta+h)}{\cosh \frac{(2n+1)\pi}{a_1}h} \qquad (87a)$$

$$\Omega_{yn}(\zeta) = \frac{4a_2}{\pi^2(2n+1)^2} \frac{\cosh \frac{(2n+1)\pi}{a_2}(\zeta+h)}{\cosh \frac{(2n+1)\pi}{a_2}h} \qquad (87b)$$

$$H_n(\omega) = \frac{1}{\Lambda_n^2 - \omega^2} \qquad (87c)$$

where a_1, a_2, and h are the dimensions of the tank along the x- and y-axes and the height of the fluid, respectively, and Λ_n is the nth natural slosh frequency. The transformation between ζ and z is

$$\zeta = z - h \qquad (88)$$

5. NUMERICAL RESULTS

5.1 Slosh Frequencies and Tank Vibration Frequencies

The tank is assumed to be isotropic with the following material elastic properties:

Young's modulus : $E = 1250 kgf / mm^2$

Poison's ratio　　: $v=0.3$

Specific weight　: $\rho g = 1820 kg / m^3$

The slosh frequencies of a rectangular tank are given by Eq. (62). Table 5.1 lists the first sixteen slosh frequencies for the tank shown in Fig. 2.1 for two water levels h. The tank has the dimensions a_1=3.0m, a_2=2.0m, b=2.0m, and is subjected to horizontal excitation parallel to the x-axis. It is seen that the slosh frequencies corresponding to the given two water levels, h=1.0m and h=1.8m are nearly identical, except for the lowest frequency.

Table 5.2 and Figure 5.1-5.6 lists the first six natural frequencies and the vibration modes for the entire tank.

A comparison of Tables 5.1 and 5.2 shows that the slosh frequencies of the tank and the vibration frequencies of the tank are well separated. This suggests that the effects of fluid-structure interaction during vibration are minimal.

Consequently, the fluid slosh forces exerted on the tank can be computed by regarding the tank walls as rigid. Of course, the forces act on an elastic tank.

Table 5.1 Slosh frequencies (Hz)

h=1.0m

i	Λ_i	i	Λ_i
1	0.4507	9	2.1029
2	0.8817	10	2.2232
3	1.1404	11	2.3372
4	1.3494	12	2.4460
5	1.5301	13	2.5501
6	1.6916	14	2.6502
7	1.8389	15	2.7466
8	1.9753	16	2.8397

h=1.8m

i	Λ_i	i	Λ_i
1	0.4984	9	2.1029
2	0.8834	10	2.2232
3	1.1405	11	2.3372
4	1.3494	12	2.4460
5	1.5301	13	2.5501
6	1.6916	14	2.6502
7	1.8389	15	2.7466
8	1.9753	16	2.8397

Table 5.2 Natural frequencies (Hz) for the entire tank

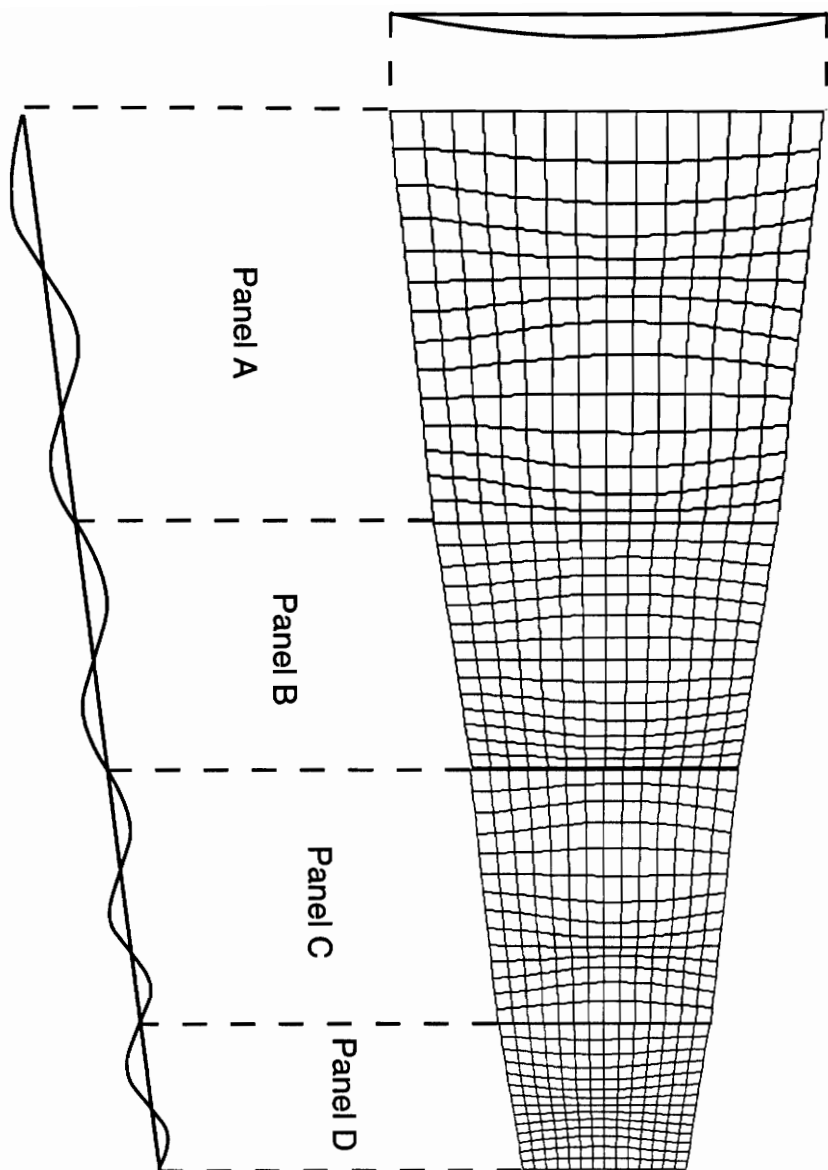| i	ω_i	i	ω_i
1	11.221702	4	19.126770
2	12.098619	5	29.656633
3	18.459779	6	30.239724

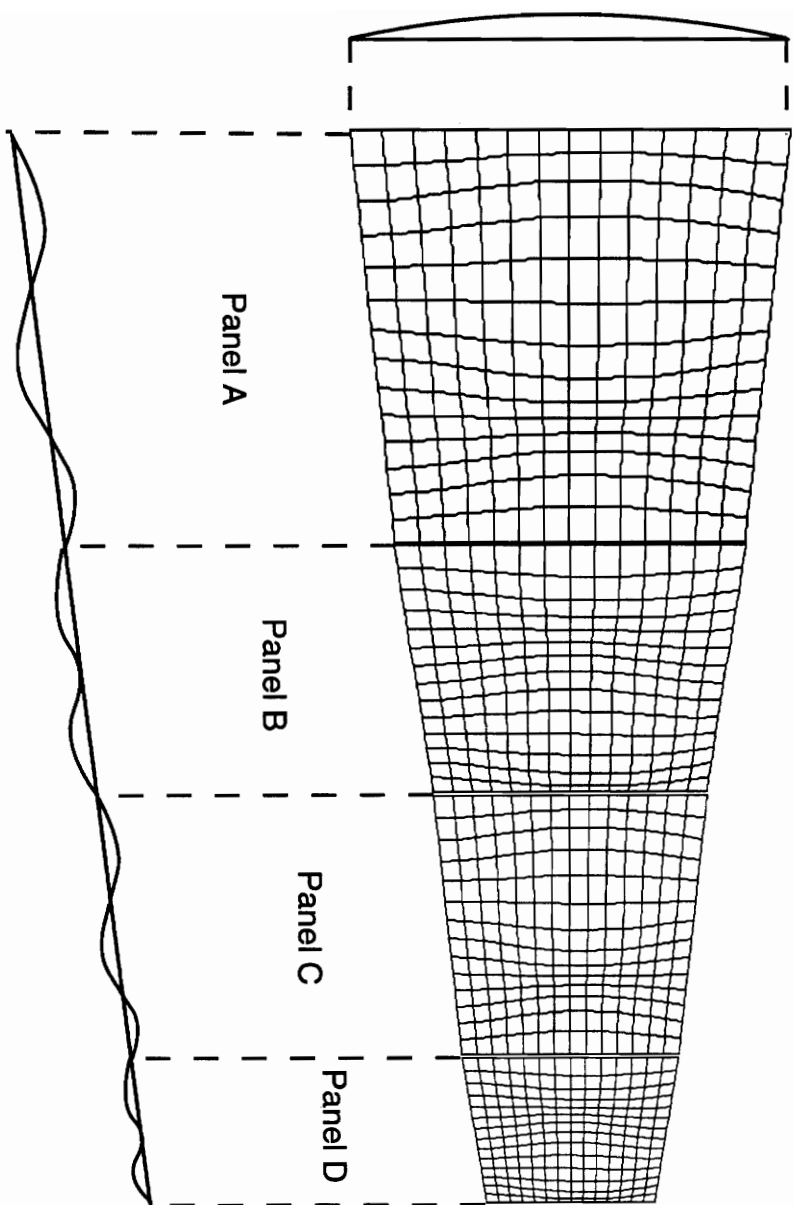Figure 5.1 The first vibration mode shape of a tank

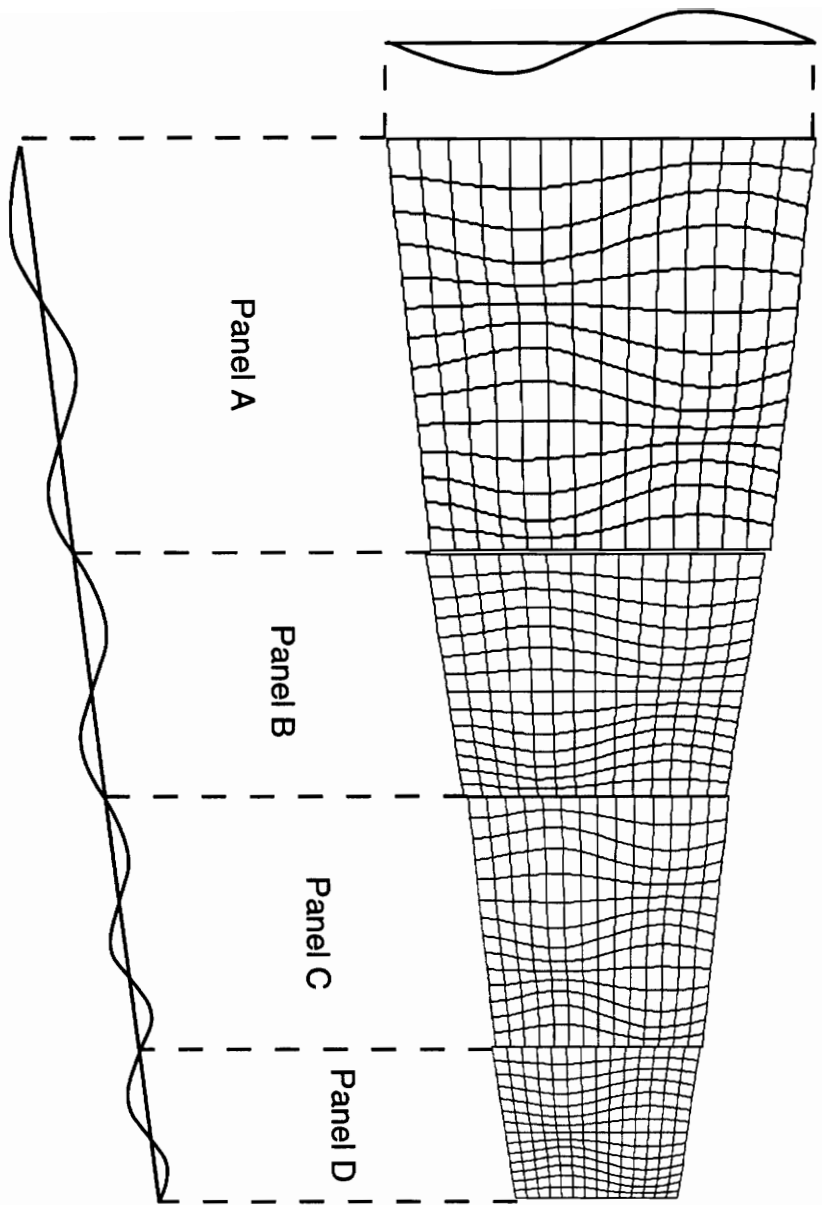Figure 5.2 The second vibration mode shape of a tank

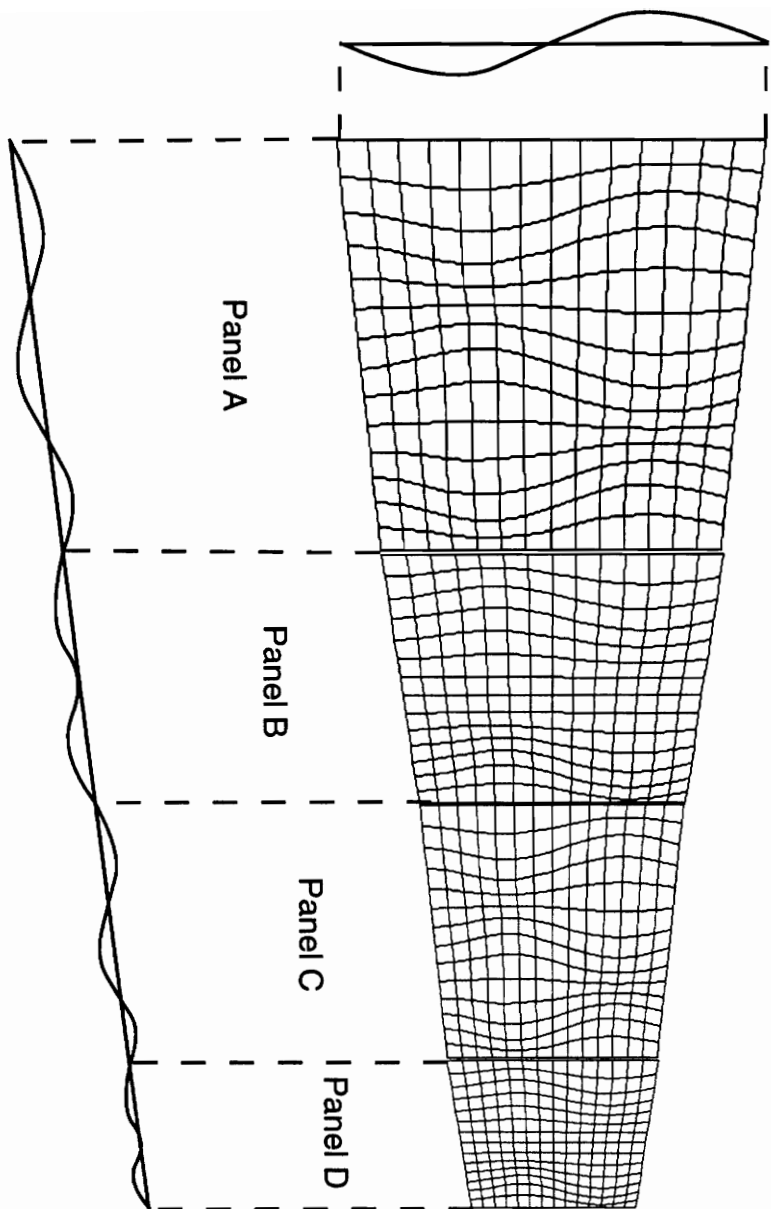Figure 5.3 The third vibration mode shape of a tank

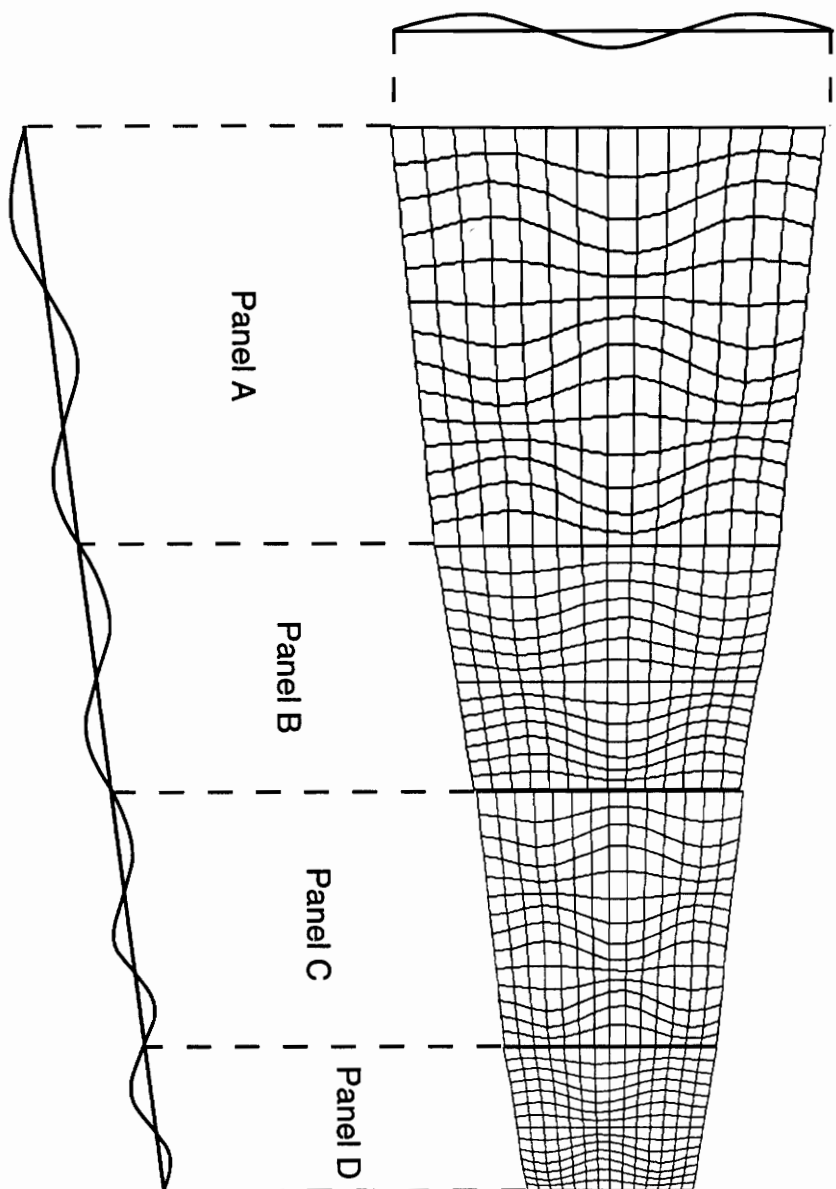Figure 5.4 The fourth vibration mode shape of a tank

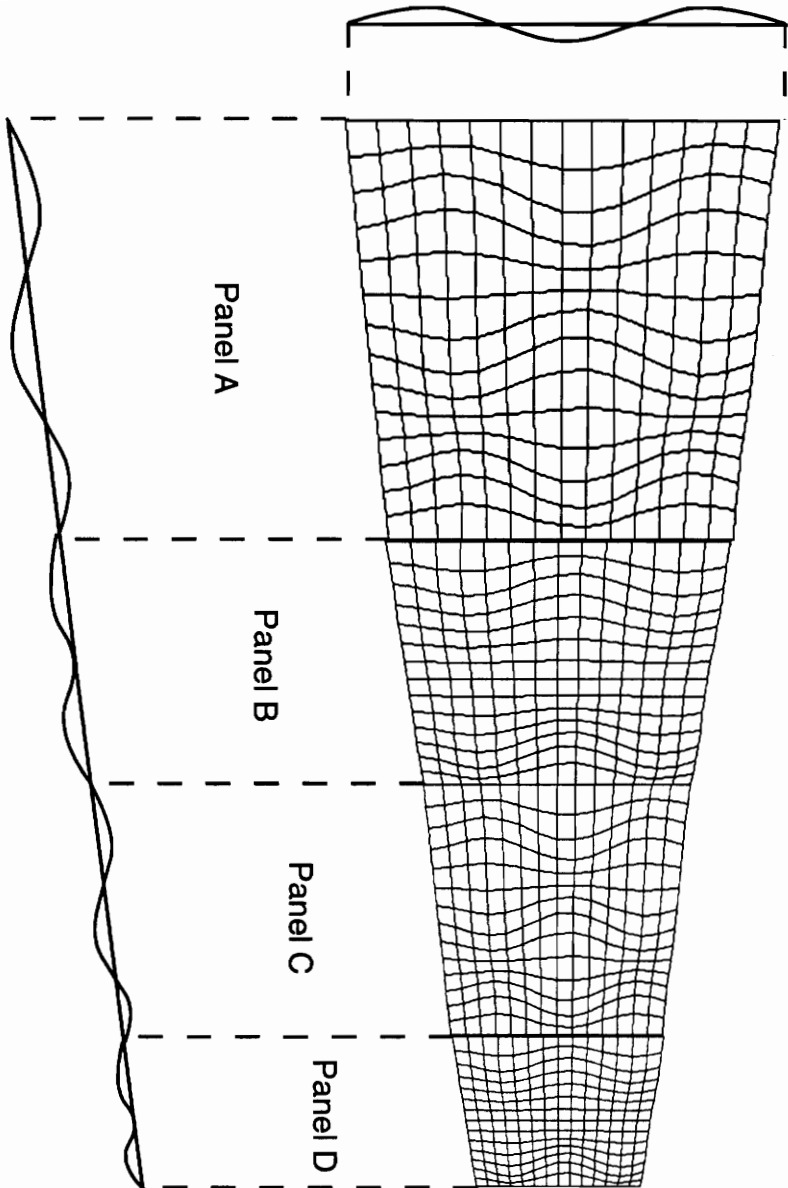Figure 5.5 The Fifth vibration mode shape of a tank

Figure 5.6 The sixth vibration mode shape of a tank

5.2 Probability of Failure of the Tank

For a given base accerelation, we can generate the principal stress mean square value at any point of the tank by means of Eq. (81). Once the principal stress probability density function has been derived, maximum principal stress theory is used to calculate the probability of failure by calculating the area to the right of the allowable stress in the Gaussian probability density function.

We use the data corresponding to an earthquake of intensity 6.9 on the Richter scale that took place on Mar 27, 1963 in Osaka, Japan. The tensile stress for the material is $3.18 \, kg / mm^2$. Table 5.3 shows the probability of failure at certain points (Figure 5.7) of a tank of dimensions $a_1=3m$, $a_2=2m$, $b=2m$, for a water level of 2m.
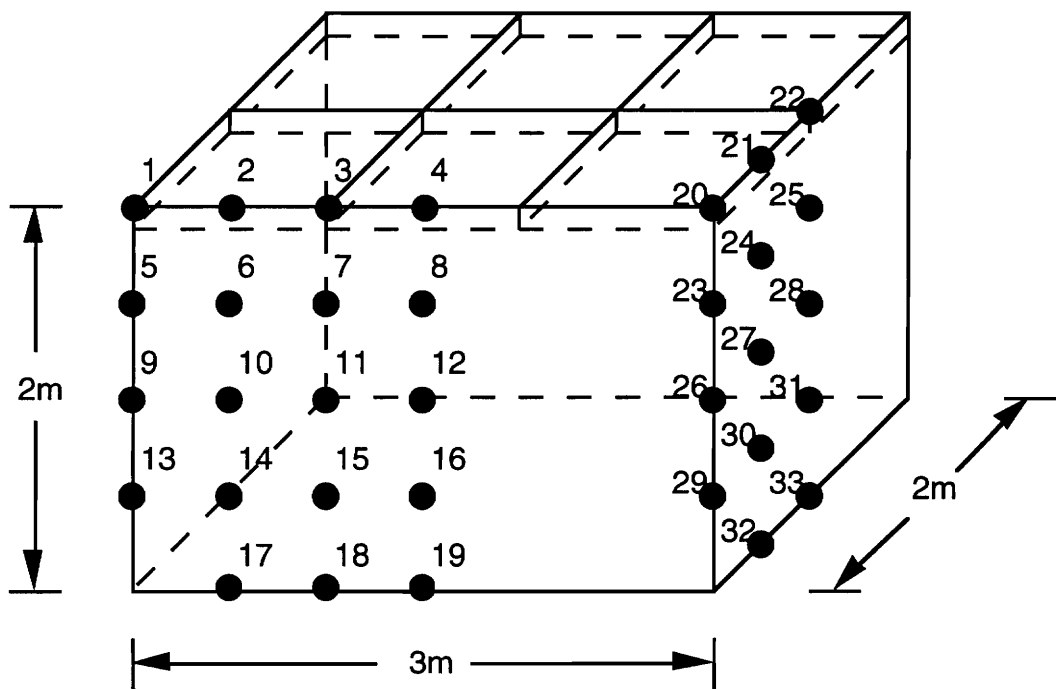

Figure 5.7 Points for which the probability of failure is predicted

Table 5.3 Probability of failure at certain points of the tank

number	failure(%)	location	number	failure(%)	location
1	0.0	(0.0,2.0)	18	0.0	(1.0,0.0)
2	0.0	(0.5,2.0)	19	0.0167997	(1.5,0.0)
3	0.0	(1.0,2.0)	20	0.0	(0.0,2.0)
4	0.0	(1.5,2.0)	21	0.0	(0.5,2.0)
5	0.0	(0.0,1.5)	22	0.0	(1.0,2.0)
6	0.0	(0.5,1.5)	23	0.0	(0.0,1.5)
7	0.0	(1.0,1.5)	24	0.0	(0.5,1.5)
8	0.0	(1.5,1.5)	25	0.0	(1.0,1.5)
9	0.0	(0.0,1.0)	26	0.0	(0.0,1.0)
10	0.0	(0.5,1.0)	27	0.0002930	(0.5,1.0)
11	0.0	(1.0,1.0)	28	0.0	(1.0,1.0)
12	0.0	(1.5,1.0)	29	0.0	(0.0,0.5)
13	0.0	(0.0,0.5)	30	0.0	(0.5,0.5)
14	0.0	(0.5,0.5)	31	0.0	(1.0,0.5)
15	0.0	(1.0,0.5)	32	0.0022614	(0.5,0.0)
16	0.0000033	(1.5,0.5)	33	0.0	(1.0,0.0)
17	0.0019544	(0.5,0.0)			

Note that the pobability of failure is zero at the upper ring and at the ribs.

6. SUMMARY AND SUGGESTIONS FOR FURTHER WORK

6.1 Summary

The tank has been modeled by substructure synthesis (ref. 4), whereby a complex structures can be regarded as an assemblage of a number of simpler structures. This method yielded a model with a relatively small number of degrees of freedom. Figures 5.1-5.6 show the first six vibration mode shapes of a tank, and note that the four panels have been unfolded for easy visualization. The top of the panel and the ribs seem to have undergone insignificant displacements.

The excitation forces are assumed to represent Gaussian random processes, defined by the mean value and standard deviation, in particular the latter. Because the relationship between the displacement and the stress is independent of time, the response principal stress is also Gaussian. Once we can derive the response principal stress, we can predict the probability of failure of the tank by means of the maximum principal stress theory (ref. 14).

Table 5.3 shows the probability of failure at certain points of the tank, and we note that the weakest points of the tank are at the bottom, i.e., points 17,19, and 32. As the maximum probability of failure is about 0.017%, which occurs at point 19, we can conclude that the entire tank is relatively strong. Still, to

decrease the probability of failure further, it is advisable to place a reinforcing ring at the bottom.

6.2 Suggestions for Further Work

We assumed that the earthquake motion is only in the horizontal direction. If we consider earthquake motions in the vertical direction, then the roof of the tank may present a problem.

The fluid pressure was treated as a one-dimensional problem. The treatment of the fluid problem is significantly more rigorous than in other investigations (e.g., ref. 1). More accuracy can be gained by regarding the problem as three-dimensional. The gains in accuracy, however , may not justify the effort.
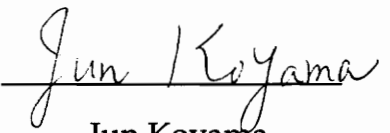
REFERENCES

1. Housner, G. W., "Dynamic Pressure on Accelerated Fluid Containers," *Bulletin of the Seismological Society of America*, Vol. 47, No.1, January 1957.

2. Abramson, H. N., "The Dynamic Behavior of Liquids in Moving Containers," *NASA SP-106*, National Aeronautics and Space Administration, Washington, D. C., 1966.

3. Bauer, H. F., Hsu, T. M., and Wang J. T. S. , "International of a Sloshing Liquid with Elastic Containers," *Journal of Basic Engineering, ASME*, Vol. 90, September, 1968, pp. 373-377. Journal of Engineering for Industry, ASME,

4. Meirovitch, L. and Kwak, M. K., "Rayleigh-Ritz Based Substructure Synthesis for Flexible Multibody Systems," *AIAA Journal*, Vol. 29, No. 10, 1991, pp. 1709-1719

5. Hurty, W. C., "Vibrations of Structural Systems by Component-Mode Synthesis," *Journal of the Engineering Mechanics Division, ASCE*, Vol. 86, Aug. 1960, pp. 51-69.

6. Hurty, W. C., "Dynamics Analysis of Structural Systems Using Component Modes," *AIAA Journal*, Vol. 3, No. 4, 1965, pp. 678-685.

7. Meirovitch, L., "A Stationary Principle for the Eigenvalue Problem for Rotating Structures," *AIAA Journal*, Vol. 14, No. 10, 1976, pp. 1387-1394

8. Meirovitch, L. and Hale, A. L., "Synthesis and Dynamic Characteristics of Large Structures with Rotating Substructures," *Proceedings of the IUTAM Symposium on the Dynamics of Multibody Systems*. (Editor: K. Magnus), Springer-Verlag, Berlin, 1978, pp. 231-244.

9. Meirovitch, L. and Hale, A. L., "On the Substructure Synthesis Method," *An International Conference on Recent Advances in Structural Dynamics*, Southampton, England, 7-11 July, 1980.

10. Meirovitch, L. and Kwak, M. K., "On the Convergence of the Classical Rayleigh-Ritz Method and the Finite Element Method," *AIAA Journal,* Vol. 28, No. 8, 1990, pp. 1509-1516

11. Meirovitch, L., *Computational Methods in Structural Dynamics,* Sijthoff & Noordhoff, The Netherlands, 1980

12. Newland, D. E., *An Introduction to Random Vibration and Spectral Analysis,* Longman, New York, 1975

13. Lamb, H., *Hydrodynamics,* Dover Publication, 1945

14. Ugural, A. C., *Stresses in Plates and Shells,* McGraw-Hill, New York, 1981

15. Meirovitch, L., *Methods of Analytical Dynamics,* McGraw-Hill, New York, 1988

16. Meirovitch, L., *Analytical Methods in Vibrations,* The Macmillan Co., New York, 1972

17. Ghali, A. and Neville, A. M., *Structual Analysis,* International Textbook Co, 1972

VITA

The author was born on December 31, 1968, in Osaka, Japan. He received the degree of Bachelor of Science in Electrical Controlled Mechanics of Engineering from Osaka University in March 1990. Taking advantage of an opportunity to attend graduate school in the USA, the author arrived in Blacksburg in July 1990. In January 1991 he entered Virginia Polytechnic Institute and State University to study for the degree of Master of Science in Engineering Mechanics . He expects to work for the degree of Ph. D. in Japan.

Jun Koyama